Bioorganic & Medicinal Chemistry Letters 22 (2012) 7742–7747

Contents lists available at SciVerse ScienceDirect

Bioorganic & Medicinal Chemistry Letters

journal homepage: www.elsevier.com/locate/bmcl

Structure based medicinal chemistry approach to develop 4-methyl-7-deazaadenine carbocyclic nucleosides as anti-HCV agent

Anandarajan Thiyagarajan [a], Mohammed T. A. Salim [b], Tuniki Balaraju [a], Chandralata Bal [a,*], Masanori Baba [b], Ashoke Sharon [a,*]

[a] Department of Applied Chemistry, Birla Institute of Technology, Mesra, Ranchi 835215, India
[b] Division of Antiviral Chemotherapy, Center for Chronic Viral Diseases, Graduate School of Medical and Dental Sciences, Kagoshima University, 8-35-1, Sakuragaoka, Kagoshima 890-8544, Japan

ARTICLE INFO

Article history:
Received 30 July 2012
Revised 16 September 2012
Accepted 19 September 2012
Available online 13 October 2012

Keywords:
Hepatitis C Virus
Carbocyclic nucleoside
Nucleoside inhibitor
Drug like properties
Molecular modelling

ABSTRACT

The structure-based approaches were implemented to design and rationally select the molecules for synthesis and anti-HCV activity evaluation. The systematic structure–activity relationships of previously discovered molecules (types **I**, **II**, **III**) were analyzed to design new molecules (type **IV**) by bioisosteric replacement of the amino group. The ligand conformation, binding mode studies and drug like properties were major determinant for selection of molecules for final synthesis. The replacement of amino group with methyl restored the interactions with RNA-template (Tem 799) through bifurcated weak H-bond (C–H. . .O). This is an interesting finding observed from molecular modeling studies. It was found that **6c–e** has anti-HCV activity (EC_{50} in 37–46 μM) while **6a, 6b** and **6g** were inactive. The compound **6f** (EC_{50} 28 μM) was the most active among the series however it also showed some cytotoxicity (CC_{50} 52.8 μM). Except **6f**, none of the compounds were found to be cytotoxic (CC_{50} > 100 μM). The present study discloses structure–based approach for novel anti-HCV lead discovery and opens a future scope of lead optimization.

Hepatitis C virus (HCV), a member of *Flaviviridae* family is now considered under major health threat with more than 200 million infected individuals worldwide.[1] In addition, long-term infection can lead to chronic liver disease, such as cirrhosis of the liver or hepatocellular carcinoma. Current standard therapy involving combination of interferon-alpha (IFN-α) and ribavirin has limited efficacy and is associated with significant side-effects even when used with the newly approved HCV protease inhibitors telaprevir and boceprevir. Therefore, there is a need for more effective anti-HCV agents that can be used in IFN-α/ribavirin sparing regimens.[2] An ideal therapy against hepatitis C is expected to have a broad spectrum of activity against all HCV genotypes, shorten treatment duration, minimal side effects and a high barrier to resistance. The HCV non-structural (NS) protein NS5B RNA-dependent RNA polymerase (RdRp) is a key component of the replicative complex and is responsible for initiating and catalyzing viral RNA synthesis.[3,4] Nucleoside analogues continue to play a vital role in the search for improved therapies for HCV infection. Nucleosides that target HCV RdRp have demonstrated advantages of broader activity against various HCV genotypes and a higher barrier to development of resistant viruses when compared to known HCV protease inhibitors.[5] The recent report on anti-HCV compound discloses various structural modifications of nucleosides either on sugar or on the base to discover new agents (Fig. 1) with improved efficacy and safety over existing drugs.[6–11]

Introduction of a 2′-CH_3 to the sugar ring of adenosine, the natural substrate, yielded highly potent type **I** molecule (Fig. 1).[8] Further, keeping the modification of sugar constant and applying bioisosteric replacement of 7-N with 7-CH generated equally or even more potent inhibitors (type **II** molecules).[8] An interesting induction of bioisosteric replacement of oxygen with methylene of sugar ring of type **II** resulted a new class of molecules (type **III**) recognized as carbocyclic nucleosides. This modification didn't show significant impact on biological profile but was able to maintain moderate activity. However, the glycosidic bond of carbocyclic nucleosides are resistant to nucleoside phosphorylase as well as nucleoside hydrolase and is more stable towards metabolic degradation in comparison to natural nucleoside.[12] Due to these features, carbocyclic nucleosides have received much attention as potential chemotherapeutic agents.[13–16]

These structure–activity (Fig. 1) understanding studies provided us a rational basis of structural modification to design newer analogs for better drug like profile. In the present investigation we have done bioisosteric replacement of the exocyclic amino group of type **III** with a methyl group to generate type **IV** molecules. From the various possible 7-substituted analogs, five were selected for

* Corresponding author.
E-mail addresses: cbal@bitmesra.ac.in (C. Bal), asharon@bitmesra.ac.in (A. Sharon).

0960-894X/$ - see front matter © 2012 Elsevier Ltd. All rights reserved.
http://dx.doi.org/10.1016/j.bmcl.2012.09.072

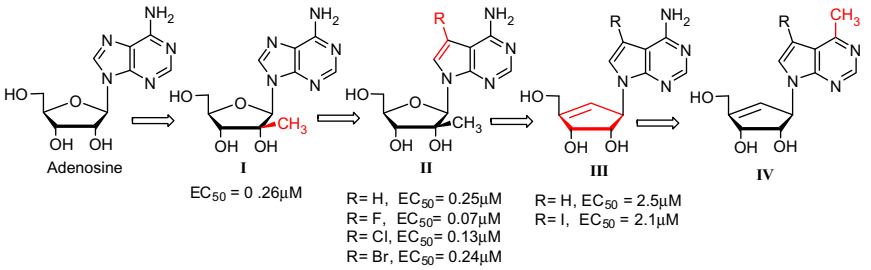

Figure 1. The chemical structure of newly discovered anti-HCV molecules (**I**-**III**). The arrow indicates stepwise modifications (indicated with red). Type **IV** is the prototype molecules designed and selected for present investigation.

synthesis on basis of a novel approach using conformational fundamental of nucleoside analogs in free-state as well as in receptor-complex.

We have recently developed the catalytic model of HCV RdRp complex[17] using the apo structure (1gx6) of HCV RdRp. The model structure comprises the complex with short template-primer chain along with the two metal ions (Fig. 2a).

The template, primer and metal ions has been extracted from published crystal structure of HIV-RT[18] to incorporate into HCV RdRp utilizing the information from recently published crystal structure of HCV RdRp complex.[19] The HCV RdRp-ATP interaction mode was more closely studied (Fig. 2b) and its understanding was imposed to our designed molecules (type **IV**) to select final molecules for synthesis. The Figure. 2b shows base pairing with template (black block: Tem799) by hydrogen bond (pink dotted line). Two metal ions MG699 and MG599 interact via metal coordinate bond (gray solid line) with Pα and Pγ phosphate respectively. The triphosphate motif was found to strongly held by polar residues Arg158, Arg48, and Lys51 through H-bonding (pink solid line and pink dotted line). The triad of aspartic acid (Asp318, Asp319 and Asp225) was found close to Pα and sugar motif of ATP. Asp 225 forms H-bonding with 3′-OH of sugar ring. The hydrophobic residues Gly 317, Phe 193, Phe 224, Cys 223, Ile 160 were found to closely associated with ATP binding. Further, hydrophilic residues Ser 288, Thr 287, Asn 291, Asn 316, Thr 221 and Ser 282 were also observed to closely interact with ATP.

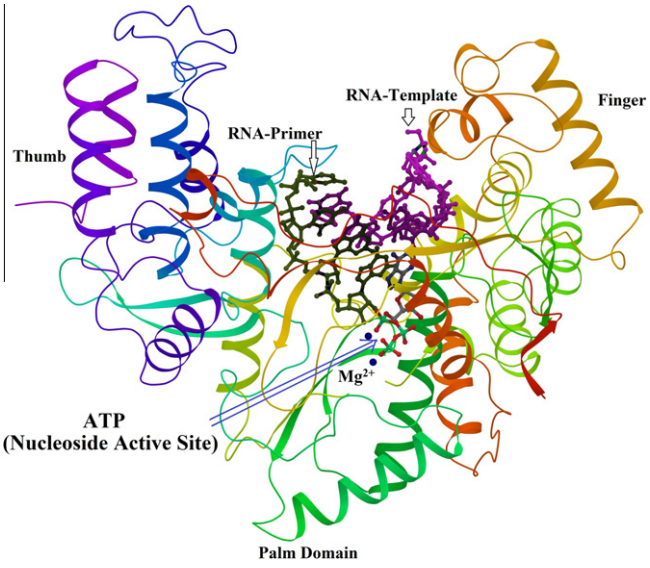

Figure 2a. A model structure of HCV RdRp with RNA double strand (primer and template), adenosine triphosphate (ATP) and two metal ions, highlighting the position of nucleoside active site.

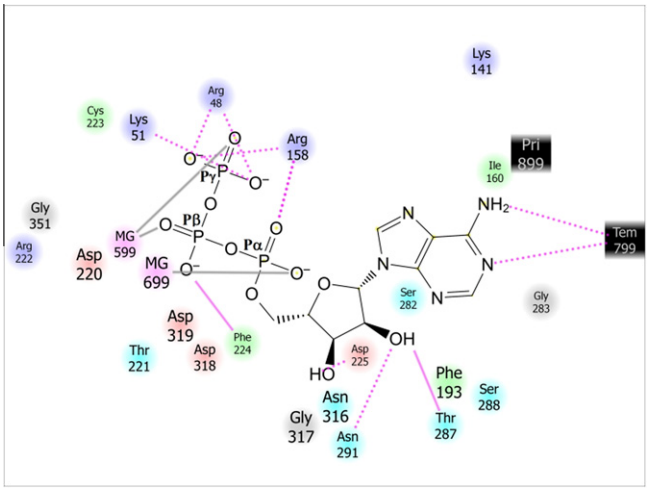

Figure 2b. Interaction profiles of ATP with HCV RdRp.

Most of the antiviral nucleoside analogs are metabolized to the corresponding nucleoside 5′-triphosphate by cellular enzymes to behave as alternative substrates for the viral polymerase followed by the nucleic acid chain termination. Therefore the modelling calculations were conducted on triphosphate form of natural substrate (adenosine) as well as our designed molecules.

The structural study of HCV RdRp-ATP complex (Fig. 3a) defines the key point related to molecular recognition motif of nucleoside binding; (i) two metal ions (Mg^{2+}) placement by interaction with Asp 220, Asp 318 and triphosphate motif of ATP; (ii) triphosphate motif conformationally positioned through H-bonding mediated by basic residues (Arg 48, Lys 51 and Arg 158); (iii) interaction of one of the Mg^{2+} with 3′-OH of primer and Pα possibly catalyzes viral RNA (vRNA) elongation through formation of 3′-O…Pα bond; (iv) HCV RdRp complex is stabilized by formation of π…π stacking (RNA primer) and strong H-bonding (pink dotted line, RNA template) between incoming nucleotide (here ATP); (v) ATP was found to be in 2′-exo conformation along with anti-disposition of base, forming H-bond pairing with RNA-template describes the importance of anti-conformation of nucleoside. Thus, the discussed features were considered as the basic recognition requirement to analyze newly designed molecules. We started with analyzing the conformations of designed molecules at nucleoside level. The conformational search was carried out for the designed molecules and top conformer was chosen for superposition with adenosine. Figure 3b shows the conformational analysis of **6a** (shown in brown), which satisfy the critical conformational requirement of molecules to fit into the nucleoside active site. Overall the main conformational feature such as anti base-disposition and 2′-exo were found significantly same for **6a** in comparison to natural substrate (adenosine: natural atom colour), however the marginal difference were observed in 5′-OH and 4′-puckering.

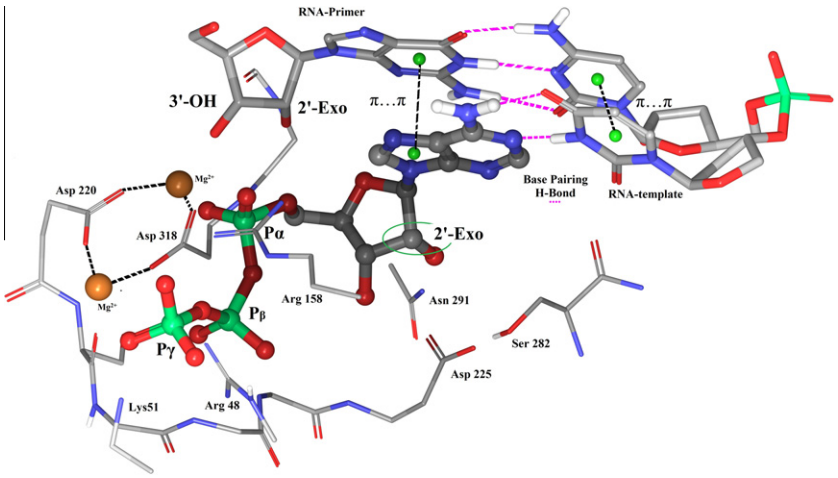

Figure 3a. HCV RdRp complex shows the binding mode of ATP and highlights the major catalytic non-covalent interaction profiles.

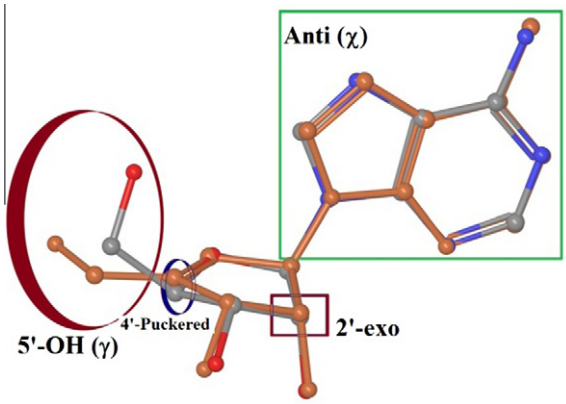

Figure 3b. The superposition of top conformation of adenonsine (natural atom colour) and **6a** (brown).

Conformational and superposition analysis for rest of the molecules were done similarly and selected molecules (Table 1) were further analyzed by molecular docking of their triphosphate form to understand the binding mode. The electrostatic surface diagram and docked complex for triphosphates were generated to investigate the possibility to fit into the nucleoside active site of HCV RdRp. Figs. 4a and 4b shows electrostatic surface and docked complex diagram for **6e** respectively**.**

It is evident from Figure 4a that the triphosphate motif occupies the basic cavity (blue), the base motif and carbocyclic sugar fits near to RNA, where a mixed pattern of acidic and hydrophobic surfaces were found. The interaction figure (Fig. 4b) highlights the major non-covalent interactions similar to previously discussed binding profile of ATP (see Fig. 3a). As the 7-NH_2 is replaced with a methyl group in **6e**, the strong H-bonding with RNA-template (Tem 799) was lost. However, the methyl group was able to form a bifurcated weak H-bond (C–H. . .O) with template. This is an interesting finding observed from molecular docking studies. Only X-ray crystal structure of designed molecule with HCV RdRp can help to confirm this observation, which is beyond the scope of current manuscript.

Glide[20] of Schrodinger Suite[21] was used for molecular docking to investigate the binding mode and docking score. Overall the docking score (Table 1), conformational similarities (Figs. 3b and 4a) and binding mode (Fig. 4b) were chosen as major rational for selection of molecules for synthesis and anti-HCV activity evaluation. The drugs like properties (DLP) were estimated using QikProp

Table 1
In-silico binding analysis and drug like properties (DLP) of analogs selected for synthesis

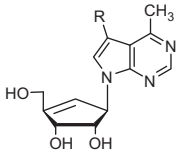

R	Molecular docking Score[a]	MM-GBSA score[b]	DLP violation[c]	
	Glide score[a]	DG	#5[d]	#3[e]
H	−12.15	−125.8	0	0
F	−13.54	−121.2	0	0
Cl	−13.56	−134.6	0	0
Br	−13.57	−132.4	0	0
I	−13.64	−130.8	0	0
–CH=CH_2	−13.53	−125.8	0	0
–C≡CH	−13.73	−125.6	0	0

[a] Glide score (G-score): The minimized poses are rescored using Schrödinger's proprietary GlideScore scoring function and the binding affinity can be estimated by G-score.

[b] MM-GBSA Score: DG = *E*_complex(minimized) − [*E*_ligand (from minimized complex) + *E*_receptor]; DG is the ligand/receptor interaction energy of the complex.

[c] DLP: Drug Like Properties.

[d] #5: Number of violations of Lipinski's rule of five. The rules are: molecular weight MW <500, QPlogPo/w <5, donorHB ⩽5, accptHB ⩽10. Compounds that satisfy these rules are considered drug-like.

[e] #3: Number of violations of Jorgensen's rule of three. The three rules are: QPlog*S* > −5.7, QPPCaco >22 nm/s, primary metabolites <7. Compounds with fewer violations of these rules are more likely to be orally available.

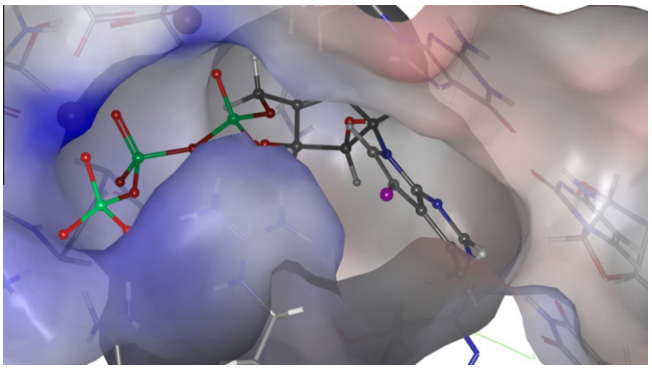

Figure 4a. The electrostatic surface diagram showing the binding of triphosphate of **6e** into the nucleoside active site.

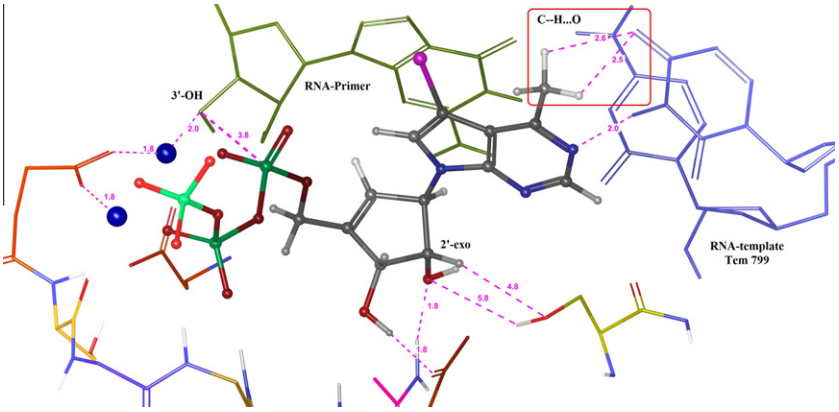

Figure 4b. The docked complex of **6e** into HCV RdRp showing a detail binding profile.

module of Schrödinger Software Suite for the selected molecules (Table 1). None of the molecules violated Lipinski's rule[22] of five as well as Jorgensen's rule[23,24] of three. Thus, the present modelling studies support the selection of analogs for final synthesis

The modified carbocyclic sugar (**1**) as a single isomer, was prepared as per earlier reported procedure[25] in eight steps from commercially available D-ribose with some optimization. During, trityl protection, DCM and DMF mixture (4:1) was used in place of DMF, which reduced the reaction time from 48 h to 12 h and made work up easier. In the TBS protection step, DMAP was used in catalytic amount using single solvent DCM. Thus, the improved procedure was able to provide 15% overall purified yield of carbocyclic sugar key intermediate **1** starting from D-ribose (Scheme 1). The optical rotation of **1** was found to be +30.9 ($[\alpha]_D^{29}$), which is close to the reported value of +28.4 ($[\alpha]_D^{23}$).[26]

4-Chloro-7*H*-pyrrolo[2,3-*d*]pyrimidine (**2**) was purchased from CiVenti Chem (India) Private Limited. The cross coupling reaction strategy[27] was applied using trimethylaluminium and $Pd(Ph_3P)_4$ catalysis to generate 4-methyl-7*H*-pyrrolo[2,3-*d*]pyrimidine (3a, Scheme 2). The Cl/Br/I was successfully introduced at C-7 of **3a** through reaction with respective *N*-halosuccinimide in DMF to generate **3c–e**. The introduction of fluoro group was a three step procedure. In brief, **2** was first treated with *N*-bromosuccinimide to introduce bromo group at C-7 (**4**), which was replaced with fluoro (**5**) by reaction with NFSI and *n*-BuLi followed by cross coupling with trimethylaluminium to yield **3b**.

Mitsunobu coupling of **1** with **3a–e** yielded protected coupled products, which were isolated, purified and deprotected to yield desired final compounds **6a–e** (Scheme 3).[28] Heck reaction was utilized for the synthesis of **6f**[29] and **6g**[30] as described in Scheme 4 with modification to earlier reported procedure.[10] In brief, **6e** was utilized as starting aryl halide and tributylvinyltin (for **6f**) or trimethylsilylacetylene (for **6g**) to introduce vinyl or ethyne group respectively.

Reaction of tributyltin directly yielded the desired product while reaction of trimethylsilylacetylene yielded the trimethylsilylated derivative, which was purified and deprotected by stirring with K_2CO_3 in methanol at room temperature.

The anti-HCV assay of **6a–g** was carried out in subgenome HCV RNA replicon cells containing the luciferase gene. The anti-HCV activity of compounds was determined by reduction of luciferase activity, while the cytotoxicity was evaluated by a tetrazolium dye method. From the dose-dependent study results (data not shown), EC_{50} (50% effective concentration) and CC_{50} (50% cytotoxic

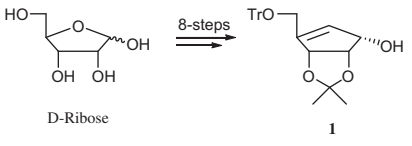

Scheme 1. Synthetic strategy for the preparation of carbocyclic sugar key intermediate **1** from D-ribose.

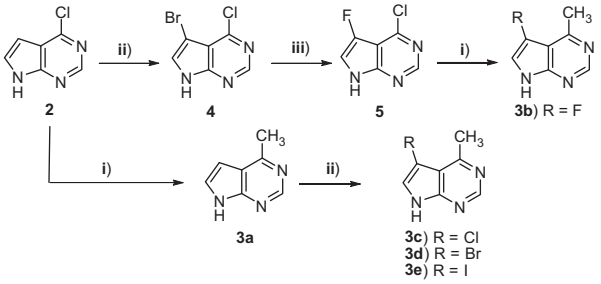

Scheme 2. Reagents and conditions: (i) $Pd(Ph_3P)_4$, $Al(CH_3)_3$, THF, 75 °C, 8 h; (ii) *N*-halosuccinimide, DMF, rt, 10 h; (iii) *n*-BuLi, NFSI, THF, −78 °C, 2 h.

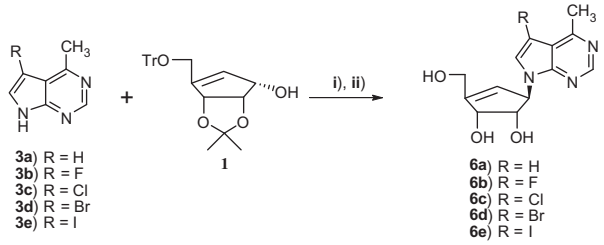

Scheme 3. Reagents and conditions: (i) Ph_3P, DIAD, THF, 0–5 °C, 2 h; (ii) 10% HCl in CH_3OH, 60 °C, 5 h.

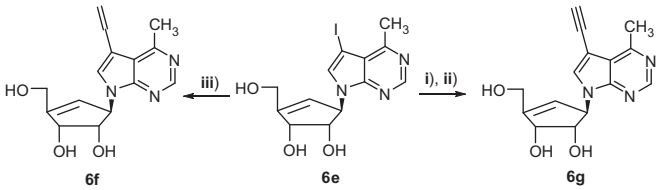

Scheme 4. Reagents and conditions: (i) $Pd(PPh_3)_4$, CuI, trimethylsilylacetylene, Et_3N, DMF, rt, 10 h; (ii) K_2CO_3, CH_3OH, rt, 4 h; (iii) $Pd(PPh_3)_4$, CuI, tributylvinyltin, Et_3N, DMF, 50 °C, 6 h.

Table 2
Anti-HCV activity of synthesized compounds

Compound	EC_{50}[b] in μM	CC_{50}[a] in μM
6a	> 100	>100
6b	> 100	> 100
6c	41.7	>100
6d	37.3	>100
6e	46.2	>100
6f	28.0	52.8
6g	67.7	>100
KZ-16	0.17	> 10

[a] The 50% cytotoxic concentration, determined by the reduction of viable cell number.
[b] The 50% effective concentration, determined by the inhibition of luciferase activity.

concentration) were calculated, and they are summarized in Table 2. KZ-16 was used as a reference compound, which has been recently reported to have selective anti-HCV activity.[31]

From the results, it was found that **6c–e** have some anti-HCV activity (Fig. 5) while **6a**, **6b** and **6g** were inactive. The compound **6f** was the most active among the series; however it also showed significant cytotoxicity. Except for **6f**, none of the compounds were found to be cytotoxic with CC_{50} values >100 μM.

Most of the molecular modeling studies were conducted on updated version of Schrödinger suite.[21] The first unliganded structure of HCV polymerases has been published[32] in 1999. Later crystal structure studies[33] with nucleoside triphosphate (NTP) form of natural substrate revealed the presence of conserved aspartic acids along with the catalytic Mg^{2+} ion (di-metal ion mechanism)[34] in the active site. The findings were previously seen in the crystal structure of HIV-RT.[18] The Prime[35] module has been used to built the model structure of HCV RdRp complex[17] using apo structure (pdb: 1gx6)[32] and HCV RdRp crystal structure (pdb: 4E7A).[19] The template, primer and metal ion has been extracted from the crystal structure of HIV-RT (1RTD; HIV polymerase + template + primer + Mg^{2+} + natural substrate)[18] to incorporate into our model structure of HCV RdRp complex. A similar right hand structure (Fig. 2a: fingers, palm, and thumb subdomains)[36] were assigned for the modeled structure with respect to HIV RT. The model structure was optimized and prepared using Protein Preparation Wizard (PPW) module of Maestro interface. The obtained structure was submitted for a short minimization through Impref module of PPW followed by a MacroModel[37] minimization employing OPLS2005 force field with 5000 iterations. A dynamic simulation of 5 ns was performed through Desmond[38] in explicit solvent system to observe the stability of HCV RdRp complex system. The average structure was minimized through MacroModel to generate the final model structure (Fig. 2a). The 3D structures of all preliminary designed molecules (Type **IV**) and their triphosphate forms were built using Maestro and treated in LigPrep to optimized ligand conformer. The conformational search was conducted through MacroModel using MMFFs force field to obtain the most favored conformations. The lowest energy conformer was selected to perform molecular docking studies. Receptor grid was generated around ATP (the natural nucleoside triphosphate) using Glide receptor grid generation utility. The docking of triphosphate form of ligands at the predefined receptor grid were conducted using XP (extra precision) mode of Glide[20] to investigate the binding mode and binding score. The docked poses were rescored using Prime[35] with MMGBSA free energy of binding, which includes ligand-HCV RdRp interaction energy (DG: Table 1). The MMGBSA scoring is based on the difference between the energy of the ligand bound complex and sum of the energy of unbound HCV RdRp [$E_{binding} = E_{complex} - (E_{protein} + E_{ligand})$]. The lowest energy conformer of all selected molecules (Table 1) was submitted for drug like properties analysis using QikProp module of Schrodinger.

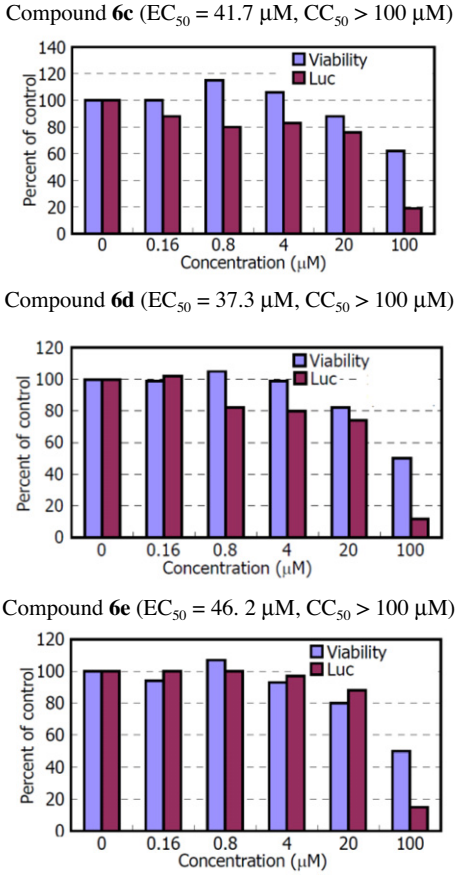

Figure 5. Anti-HCV activity of **6c–e** in replicon cells.

All compounds were dissolved in dimethyl sulfoxide (DMSO) at a concentration of 20 mM or higher to exclude the cytotoxicity of DMSO and stored at −20 °C until use. Huh-7 cells containing self-replicating subgenomic replicons with a luciferase reporter, LucNeo#2,[39] were grown and cultured in Dulbecco's modified Eagle medium with high glucose (Gibco/BRL) supplemented with 10% heat-inactivated fetal bovine serum (Gibco/BRL), 100 U/ml penicillin G, and 100 μg/ml streptomycin. LucNeo#2, were maintained in culture medium containing 1 mg/ml G418 (Nakarai Tesque). The anti-HCV activity of the test compounds was determined in LucNeo#2 cells by the previously described method with some modifications.[40] Briefly, the cells (5×10^3 cells/well) were cultured in a 96-well plate in the absence of G418 and in the presence of various concentrations of the compounds. After incubation at 37 °C for 3 days, the culture medium was removed, and the cells were washed twice with phosphate-buffered saline (PBS). Lysis buffer was added to each well, and the lysate was transferred to the corresponding well of a non-transparent 96-well plate. The luciferase activity was measured by addition of the luciferase reagent in a luciferase assay system kit (Promega) using a luminometer with automatic injectors (Berthold Technologies). The number of viable cells was determined by a dye method using the water soluble tetrazolium Tetracolor One® (Seikagaku Corporation), according to the manufacturer's instructions.

We have applied ligand-based bioisosteric replacement approach to design a new series of carbocyclic nucleoside where amino group at C-4 position (well known for H-bonding with RNA template) was replaced with a methyl group. The rational behind this approach was that the methyl group should be able to restore H-bonding through weak C–H...O interaction, which was observed in modeling studies. Although, this approach didn't yield any

highly active molecules, however, **6c–e** was found to be moderately active against HCV. The major advantages of these compounds are; limited cytotoxicity ($CC_{50} > 100\ \mu M$) and better lipophilicity. Further synthetic exploration and biological evaluation are warranted to optimize this novel lead into potential anti-HCV nucleoside inhibitor.

Acknowledgments

This research received funding from DST, New Delhi, India through grant no SR/FT/CS-069/2009. A.T. and T.B. are thankful to DST, India for JRF. AS thanks DBT, New Delhi, India for modelling software support. A.S. & C.B. would like to dedicate this manuscript to Professor C. K. Chu. Authors acknowledge ILS, Hyderabad for NMR-Mass Facility and CIF, BIT Mesra for analytical support.

Supplementary data

Supplementary data associated with this article can be found, in the online version, at http://dx.doi.org/10.1016/j.bmcl.2012.09.072.

References and notes

1. Lavanchy, D. *Clin. Microbiol. Infect.* **2011**, *17*, 107.
2. Di Bisceglie, A. M.; McHutchison, J.; Rice, C. M. *Hepatology* **2002**, *35*, 224.
3. Lavanchy, D. *Liver Int.* **2009**, *29*, 74.
4. Ishii, K.; Tanaka, Y.; Yap, C. C.; Aizaki, H.; Matsuura, Y.; Miyamura, T. *Hepatology* **1999**, *29*, 1227.
5. McCown, M. F.; Rajyaguru, S.; Le Pogam, S.; Ali, S.; Jiang, W. R.; Kang, H.; Symons, J.; Cammack, N.; Najera, I. *Antimicrob. Agents Chemother.* **2008**, *52*, 1604.
6. Carroll, S.; Olsen, D. *Infect. Disord. Drug Targets* **2006**, *6*, 17.
7. Eldrup, A. B.; Allerson, C. R.; Bennett, C. F.; Bera, S.; Bhat, B.; Bhat, N.; Bosserman, M. R.; Brooks, J.; Burlein, C.; Carroll, S. S. *J. Med. Chem.* **2004**, *47*, 2283.
8. Eldrup, A. B.; Prhavc, M.; Brooks, J.; Bhat, B.; Prakash, T. P.; Song, Q.; Bera, S.; Bhat, N.; Dande, P.; Cook, P. D. *J. Med. Chem.* **2004**, *47*, 5284.
9. Cho, A.; Saunders, O. L.; Butler, T.; Zhang, L.; Xu, J.; Vela, J. E.; Feng, J. Y.; Ray, A. S.; Kim, C. U. *Bioorg. Med. Chem. Lett.* **2012**, *22*, 2705.
10. Kim, H. J.; Sharon, A.; Bal, C.; Wang, J.; Allu, M.; Huang, Z.; Murray, M. G.; Bassit, L.; Schinazi, R. F.; Korba, B.; Chu, C. K. *J. Med. Chem.* **2009**, *52*, 206.
11. Zhang, H. W.; Zhou, L.; Coats, S. J.; McBrayer, T. R.; Tharnish, P. M.; Bondada, L.; Detorio, M.; Amichai, S. A.; Johns, M. D.; Whitaker, T.; Schinazi, R. F. *Bioorg. Med. Chem. Lett.* **2011**, *21*, 6788.
12. Crimmins, M. T. *Tetrahedron* **1998**, *54*, 9229.
13. Zhu, X. F. *Nucleosides Nucleotides Nucleic Acids* **2000**, *19*, 651.
14. Ferrero, M.; Gotor, V. *Chem. Rev.* **2000**, *100*, 4319.
15. Schneller, S. W. *Curr. Top. Med. Chem.* **2002**, *2*, 1087.
16. Wang, J.; Rawal, R. K.; Chu, C. K. *Med. Chem. Nucleic Acids* **2011**, *16*, 1.
17. Balaraju, T.; Bal, C.; Sharon, A. *Antiviral Res.* **2012**, A14.
18. Huang, H.; Chopra, R.; Verdine, G. L.; Harrison, S. C. *Science* **1998**, *282*, 1669.
19. Mosley, R. T.; Edwards, T. E.; Murakami, E.; Lam, A. M.; Grice, R. L.; Du, J.; Sofia, M. J.; Furman, P. A.; Otto, M. J. *J. Virol.* **2012**, *86*, 6503.
20. Glide-V-5.7. Schrödinger, LLC., New York, NY, **2011**.
21. Schrödinger. LLC, New York, NY, **2011**.
22. Lipinski, C. A.; Lombardo, F.; Dominy, B. W.; Feeney, P. J. *Adv. Drug Delivery Rev.* **2001**, *46*, 3.
23. Duffy, E. M.; Jorgensen, W. L. *J. Am. Chem. Soc.* **2000**, *122*, 2878.
24. Jorgensen, W. L.; Duffy, E. M. *Adv. Drug Delivery Rev.* **2002**, *54*, 355.
25. Cho, J. H.; Bernard, D. L.; Sidwell, R. W.; Kern, E. R.; Chu, C. K. *J. Med. Chem.* **2006**, *49*, 1140.
26. Ohira, S.; Sawamoto, T.; Yamato, M. *Tetrahedron Lett.* **1995**, *36*, 1537. $[\alpha]_D^{23}$ + 28.4 (*c*, 1.00, $CHCl_3$); Compound **1** $[\alpha]_D^{29}$ + 30.9 (*c*, 1.00, $CHCl_3$).
27. Hocek, M.; Pohl, R.; Císařová, I. *Eur. J. Org. Chem.* **2005**, *2005*, 3026.
28. General method for the preparation of **6a–e**.
To a mixture of appropriate **3a–e** (1.5 mmol), **1** (1.57 mmol) and Ph_3P (3.75 mmol) in THF was added DIAD (3.75 mmol) dropwise at 0 °C under nitrogen and stirring continued at rt. Completion of reaction was analyzed by TLC, solvent evaporated under reduced pressure and crude was purified by column chromatography on silica gel by eluting up to 30 % ethyl acetate in hexane to give couple products in more than 80 % yield. The deprotection was carried out by heating at 60 °C in 10 % HCl in MeOH. After completion (monitored by TLC), the reaction mixture was neutralized by $NaHCO_3$ and purified by silica gel chromatography (10% methanol in DCM) to get **6a–e** in 70–85% yield.
Data for (1*S*,2*R*,5*R*)-3-(hydroxymethyl)-5-(4-methyl-7*H*-pyrrolo[2,3-*d*]pyrimidin-7-yl)cyclopent-3-ene-1,2-diol (**6a**): Yield: 80 %; mp: 168–170 °C; MS-ESI (*m*/*z*): [M⁺+1] 261.9; $[\alpha]_D^{21}$: − 101.70 (*c* 0.24, MeOH); UV (MeOH) λ_{max} 269 nm; ^{1}H NMR (400 MHz, DMSO-d_6): δ 2.64 (s, 3H), 4.12–4.17 (m, 3H), 4.44 (t, *J* = 5.6 Hz, 1H), 4.88–4.94 (m, 2H), 5.02 (d, *J* = 7.2 Hz, 1H), 5.63–5.67 (m, 2H), 6.70 (d, *J* = 3.6 Hz, 1H), 7.43 (d, *J* = 4 Hz, 1H), 8.64 (s, 1H); ^{13}C NMR (100 MHz, DMSO-d_6): δ 21.01, 58.55, 63.90, 72.31, 77.17, 99.25, 117.59, 123.98, 126.22, 149.90, 150.16, 150.54, 158.57.
Data for (1*S*,2*R*,5*R*)-5-(5-bromo-4-methyl-7*H*-pyrrolo[2,3-*d*]pyrimidin-7-yl)-3-(hydroxymethyl)cyclopent-3-ene-1,2-diol (**6d**): Yield: 81 %; mp: 215–217 °C; MS-ESI (*m*/*z*): [M⁺] 339.8 [M⁺+2] 341.8; $[\alpha]_D^{22}$ − 130.39 (*c* 0.21 MeOH-H_2O); UV (MeOH) λ_{max} 269.8 nm, 301.7 nm; ^{1}H NMR (400 MHz, DMSO-d_6) δ 2.84 (s, 3H), 4.12–4.17 (m, 3H), 4.44 (t, *J* = 5.6 Hz, 1H), 4.88 (t, *J* = 5.6 Hz, 1H), 4.95 (d, *J* = 6 Hz, 1H), 5.06 (d, *J* = 7.2 Hz, 1H), 5.63 (d, *J* = 1.2 Hz, 1H), 5.68 (bs, 1H), 7.68 (s, 1H), 8.68 (s, 1H); ^{13}C NMR (100 MHz, DMSO-d_6) δ 21.33, 59.04, 64.71, 72.74, 77.44, 87.18, 115.77, 123.93, 126.89, 149.61, 151.22, 151.60, 159.43.
29. Method for synthesis of (**6f**).
A suspension of **6e** (0.25 mmol), $Pd(PPh_3)_4$ (0.02 mmol), CuI (0.05 mmol) and Et_3N (0.77 mmol) in anhydrous DMF was purged with nitrogen at rt. Tributylvinyltin (2.58 mmol) was added under nitrogen and the mixture was stirred at 50 °C. The completion of reaction was checked by TLC, solvent was removed and residue was purified by on silica gel (100–200 mesh) column chromatography by eluting with 10 % methanol in DCM.
Data for (1*S*,2*R*,5*R*)-3-(hydroxymethyl)-5-(4-methyl-5-vinyl-7*H*-pyrrolo[2,3-*d*]pyrimidin-7-yl)cyclopent-3-ene-1,2-diol (**6f**): Yield: 72 %; mp: 148–150 °C; MS-ESI (*m*/*z*): [M⁺+1] 287.9; $[\alpha]_D^{22}$ − 157.66 (*c* 0.11 MeOH-H_2O); UV (MeOH) λ_{max} 269.5 nm, 310.7 nm; 1H NMR (400 MHz, DMSO-d_6) δ 2.75 (s, 3H), 4.13–4.22 (m, 3H), 4.44 (t, *J* = 5.2 Hz, 1H), 4.92 (t, *J* = 5.6 Hz, 1H), 4.96 (d, *J* = 6.4 Hz, 1H), 5.06 (d, *J* = 7.2 Hz, 1H), 5.19 (d, *J* = 11.2 Hz, 1H) , 5.63 (bs, 1H), 5.63–5.68 (m, 1H), 5.63–5.68 (bs, 1H), 7.01–7.08 (m, 1H), 7.70 (s, 1H), 8.62 (s, 1H); ^{13}C NMR (100 MHz, DMSO-d_6) δ 22.85, 58.56, 63.77, 72.27, 77.13, 113.56, 113.81, 115.24, 122.86, 123.88, 128.46, 150.16, 150.22, 150.52, 158.89.
30. Method for synthesis of (1*S*,2*R*,5*R*)-5-(5-ethynyl-4-methyl-7*H*-pyrrolo[2,3-*d*]pyrimidin-7-yl)-3-(hydroxymethyl)cyclopent-3-ene-1,2-diol (**6g**)
A suspension of **6e** (0.25 mmol), $Pd(PPh_3)_4$ (0.02 mmol), CuI (0.05 mmol) and Et_3N (0.77 mmol) in anhydrous DMF was purged with nitrogen at rt. Trimethylsilylacetylene (2.58 mmol) of was added under nitrogen and the mixture was stirred at rt. The completion was checked by TLC, solvent was removed and residue was purified on silica gel (100–200 mesh) chromatography by eluting with 10 % methanol in DCM to give trimethylsilyl protected compound in 80 % yield. The deprotection was done by stirring in methanol and K_2CO_3 (0.1 mmol) at rt for 2 h and purified by silica gel chromatography by eluting up to 10 % methanol in DCM to get **6g** as a light brown solid in 75 % yield.
31. Salim, M. T.; Aoyama, H.; Sugita, K.; Watashi, K.; Wakita, T.; Hamasaki, T.; Okamoto, M.; Urata, Y.; Hashimoto, Y.; Baba, M. *Biochem. Biophys. Res. Commun.* **2011**, *415*, 714.
32. Bressanelli, S.; Tomei, L.; Roussel, A.; Incitti, I.; Vitale, R. L.; Mathieu, M.; De Francesco, R.; Rey, F. A. *PNAS* **1999**, *96*, 13034.
33. Bressanelli, S.; Tomei, L.; Rey, F. A.; De Francesco, R. *J. Virol.* **2002**, *76*, 3482.
34. Steitz, T. A.; Smerdon, S. J.; Jager, J.; Joyce, C. M. *Science* **1994**, *266*, 2022.
35. Prime-V-3.0, Schrödinger, LLC., New York, NY, **2011**.
36. Joyce, C. M.; Steitz, T. A. *J. Bacteriol.* **1995**, *177*, 6321.
37. MacroModel-V-9.9. Schrödinger, LLC., New York, NY, **2011**.
38. Desmond-V-3.0. Schrödinger, LLC., New York, NY, **2011**.
39. Goto, K.; Watashi, K.; Murata, T.; Hishiki, T.; Hijikata, M.; Shimotohno, K. *Biochem. Biophys. Res. Commun.* **2006**, *343*, 879.
40. Windisch, M. P.; Frese, M.; Kaul, A.; Trippler, M.; Lohmann, V.; Bartenschlager, R. *J. Virol.* **2005**, *79*, 13778.